ENGINEERING TRANSACTIONS • *Engng. Trans.* • **41**, 2, 139–156, 1993
Polish Academy of Sciences • Institute of Fundamental Technological Research

DETERMINATION OF DRYING INDUCED STRESSES IN A PRISMATIC BAR

A. RYBICKI (POZNAŃ)

In the paper a solution of the two-dimensional problem of convective drying of porous – capillary material is presented. The considered phenomenon is described by a system of coupled differential equations proposed by KOWALSKI [7, 8]. The problem is solved with the use of the finite element method for spatial derivatives and of the three-point finite difference method for derivatives with respect to time. The obtained results with special emphasis on the stress distributions are shown diagrammatically.

NOTATION

x, y, z [m]	coordinates of points,
t [s]	time,
u_x, u_y, u_z [m]	components of the displacement vector,
A [N/m^2]	bulk modulus for porous material,
M [N/m^2]	shear modulus for porous material,
σ_{ij} [N/m^2]	components of the total stress tensor,
ε_{ij} [1]	components of the strain tensor,
T[°K]	absolute temperature,
ϑ [deg]	relative temperature,
Θ [1]	specific moisture content,
c_ϑ [J/m^{2}deg]	thermal coefficient of the moisture potential,
c_Θ [J/m^3]	moisture content coefficient of the moisture potential,
α_ϑ [deg^{-1}]	coefficient of the linear thermal expansion,
α_Θ [1]	coefficient of the linear humidity expansion,
α_m [kg s/m^4]	coefficient of the convective mass exchange,
μ [J/kg]	moisture potential density,
Λ [W/m °K]	coefficient of thermal conductivity,
Λ_m [kg s^3/m]	coefficient of moisture conductivity,
ρ_0 [kg/m^3]	density of the skeleton of porous material.

1. Introduction

The process of drying of wet porous-capillary materials is accompanied by some changes in the shape of the body due to shrinkage. In turn, this usually gives rise to some shrinkage stresses that, similarly as the thermal stresses, are caused by internal changes in the material. Their existence is independent of the mechanical forces applied. The reasons for the generation of drying stresses is caused by: nonuniform distribution of moisture content, nonuniform distribution of temperature and a mechanical field due to external forces, if any.

Nonuniformity of the moisture content distribution increases along with the rate of drying process. The evaporation of moisture from the boundary surface proceeds faster than the flow of moisture from the interior of the dried material. That is why the shrinkage of material layers near the surface is considerably larger than that in the interior. The shrinkage stresses of the surface layers may often exceed the limit value of the strength of the material so the surface cracks and even the through cracks (leading to the damage of the whole material structure) can occur.

In the paper such shrinkage stresses in the dried material are analysed which do not exceed its strength. The elastic (reversible) stresses only are allowed for in the presented considerations. The model proposed by Kowalski [7, 8] is used for the description of the stated problem. The model relates stresses to strains, moisture content and temperature of the material and has the form of a system of five doubly coupled differential equations whose solution must additionally satisfy the compatibility relationships. The above mentioned couplings mean that a variation in one of the three fields involved, i.e. either the temperature or the moisture content or the strain field, causes mutual variations in the two remaining ones. In other models put forward in the literature on drying, e.g.[1–5], an influence of the strain field on the temperature field and the moisture distribution field was ignored.

An analysis of the generation of shrinkage stresses together with the numerical results for the distribution of shrinkage stresses was made in [10]. The paper concerned a one-dimensional case of convective drying of a plate resting on an impermeable foundation. In order to concentrate attention on the shrinkage stresses caused exclusively by the moisture content variations, the considerations were confined to the so-called first period of drying when the temperature of the dried material remained constant and equal to the temperature of the wet-bulb thermometer [6], and no external mechanical fields acted on the plate.

Similar two-dimensional problem will be dealt with in this paper. Convective drying of an infinite bar with rectangular cross-section will be considered under the same assumption as those made in [10]. The coupled system of three second-order differential equations describing the problem will be solved with the use of the finite element method. The numerical results will be shown by means of various diagrams.

2. Shrinkage stresses. Basic system of equations

The distribution of the shrinkage stresses will be determined on the basis of moisture concentration distribution (or the moisture potential), the temperature distribution and the dilatancy of the porous material in question. These fields are described by the following system of equations [8]:

$$M\nabla^2\mathbf{u} + \left(M + A - \frac{\gamma_\Theta^2}{c_\Theta}\right)\operatorname{grad}\operatorname{div}\mathbf{u} - \left(\gamma_\vartheta - \gamma_\Theta\frac{c_\vartheta}{c_\Theta}\right)\operatorname{grad}\vartheta - \frac{\gamma_\Theta}{c_\Theta^\rho}\operatorname{grad}\mu = 0,$$

$$K\nabla^2\mu = \mu + \frac{\gamma_\Theta}{\rho_0}\operatorname{div}\mathbf{u} - \frac{c_\vartheta}{\rho_0}\vartheta, \tag{2.1}$$

$$\kappa\nabla^2\vartheta = \vartheta + \kappa_E\operatorname{div}\mathbf{u} - \kappa_\Theta\mu,$$

where $\mathbf{u}$ is the displacement vector of the dried material, μ stands for the moisture potential and ϑ denotes the relative temperature. In addition, the following formulae are present in Eqs. (2.1):

$$K = \Lambda_m\frac{c_\Theta^\rho}{\rho_0}, \qquad c_\Theta^\rho = \frac{c_\Theta}{\rho_0},$$

$$\kappa_E = \frac{c_\rho - c_\vartheta}{3\alpha_\vartheta c_\vartheta}\left(1 - \frac{c_\vartheta}{c_\Theta}\frac{\gamma_\Theta}{\gamma_\vartheta}\right), \tag{2.2}$$

$$\gamma_\vartheta = (2M + 3A)\alpha_\vartheta, \qquad \gamma_\Theta = (2M + 3A)\alpha_\Theta,$$

where Λ_m is the coefficient of moisture conductivity, c_Θ is the moisture content coefficient of the moisture potential, α_ϑ, α_Θ stand for the coefficients of the linear thermal expansion and the linear humidity expansion, respectively, M, A, denote Lamé's constants for the dried material and ρ_0 is the density of dry material.

Knowing the fields $\mathbf{u}$, ϑ, μ, the distribution of the specific moisture content can be found from the formula (see [8])

$$\Theta = \Theta_r + (\rho_0\mu - c_\vartheta\vartheta + \gamma_\Theta \operatorname{div}\mathbf{u})/c_\Theta \tag{2.3}$$

followed by the stress distribution σ_{ij} associated with a given thermomechanical state and the given moisture distribution:

$$\sigma_{ij} = 2M\varepsilon_{ij} + [A\varepsilon_{kk} - \gamma_\vartheta\vartheta - \gamma_\Theta(\Theta - \Theta_r)]\sigma_{ij}\,, \tag{2.4}$$

where

$$\gamma_\vartheta = \alpha_\vartheta(2M + 3A), \qquad \gamma_\Theta = \alpha_\Theta(2M + 3A),$$

and

$$\varepsilon_{ij} = (u_{i,j} + u_{j,i})/2 \tag{2.5}$$

denotes a small strain tensor of the dried material.

During the first period of drying the temperature ϑ is equal to the temperature of the wet-bulb thermometer and remains constant. The system of Eqs. (2.1) is reduced to take the form

$$\begin{aligned} M\nabla^2\mathbf{u} + \left(M + A - \frac{\gamma_\Theta^2}{c_\Theta}\right)\operatorname{grad}\operatorname{div}\mathbf{u} - \frac{\gamma_\Theta}{c_\Theta^\rho}\operatorname{grad}\mu = 0, \\ K\nabla^2\mu = \mu + \frac{c_\Theta}{\rho_0}\operatorname{div}\mathbf{u}. \end{aligned} \tag{2.6}$$

3. Formulation of the two-dimensional problem

The problem to be solved is that of convective drying of an infinite bar having a rectangular cross-section. None of the sides of the bar is loaded and at the initial instant of time the moisture distribution in the material is uniform; in other words, the distribution of moisture content potential μ_0 is constant and no initial stresses are present. The first period of drying is considered which takes place at constant temperature equal to the wet-bulb temperature [6]. The bar is submerged in a uniform atmosphere with constant moisture potential. Drying continues in a convective manner.

Under the circumstances, the following initial-boundary problem is formulated: find such functions $u_x(x, y, t)$, $u_y(x, y, t)$, $\mu(x, y, t)$ that, within

the rectangle $(-L, L) \times (-H, H)$ and for $t \in R^+$, satisfy the system of differential equations

$$\left(2M + A - \frac{\gamma_\ominus^2}{c_\ominus}\right)\frac{\partial^2 u_x}{\partial x^2} + M\frac{\partial^2 u_x}{\partial y^2} + M\frac{\partial^2 u_y}{\partial y \partial x} + \left(A - \frac{\gamma_\ominus^2}{c_\ominus}\right)\frac{\partial^2 u_y}{\partial x \partial y} - \frac{\gamma_\ominus}{c_\ominus^\rho}\frac{\partial \mu}{\partial x} = 0,$$

$$\left(A - \frac{\gamma_\ominus^2}{c_\ominus}\right)\frac{\partial^2 u_x}{\partial x \partial y} + M\frac{\partial^2 u_x}{\partial y \partial x} + M\frac{\partial^2 u_x}{\partial x^2} + \left(2M + A - \frac{\gamma_\ominus^2}{c_\ominus}\right)\frac{\partial^2 u_y}{\partial y^2} - \frac{\gamma_\ominus}{c_\ominus^\rho}\frac{\partial \mu}{\partial y} = 0, \tag{3.1}$$

$$\frac{\gamma_\ominus}{\rho_0}\frac{\partial^2 u_x}{\partial x \partial t} + \frac{\gamma_\ominus}{\rho_0}\frac{\partial^2 u_y}{\partial y \partial t} + \frac{\partial \mu}{\partial t} - K\frac{\partial^2 \mu}{\partial x^2} - K\frac{\partial^2 \mu}{\partial y^2} = 0,$$

in the presence of the stress boundary conditions

$$\begin{aligned} \sigma_{11}|_{x=L} &= \sigma_{11}|_{x=-L} = 0, \\ \sigma_{22}|_{y=H} &= \sigma_{22}|_{y=-H} = 0, \\ \sigma_{12}|_{x=L} &= \sigma_{12}|_{x=-L} = \sigma_{12}|_{y=H} = \sigma_{12}|_{y=-H} = 0, \end{aligned} \tag{3.2}$$

for the moisture flow

$$\left.\frac{\partial \mu}{\partial x}\right|_{x=-L} = \left.\frac{\partial \mu}{\partial x}\right|_{x=L} = \left.\frac{\partial \mu}{\partial y}\right|_{y=-H} = \left.\frac{\partial \mu}{\partial y}\right|_{y=H} = -(\alpha_m/\Lambda_m)(\mu - \mu_a), \tag{3.3}$$

and in the presence of the initial conditions

$$\mu(x, y, 0) = \mu_0, \qquad \sigma_{ij}(x, y, 0) = 0, \qquad \text{for} \quad i, j = 1, 2. \tag{3.4}$$

The finite element technique will be employed to arrive at the solution sought.

4. Formulation of the FEM problem

The solution within the relevant domain will be sought in an approximate manner:

$$
\begin{aligned}
u_x(x,y,t_k) &= \sum_{n=1}^{N} a_n^1(t)\,\psi_n(x,y),\\
u_y(x,y,t_k) &= \sum_{n=1}^{N} a_n^2(t)\,\psi_n(x,y),\\
\mu(x,y,t_k) &= \sum_{n=1}^{N} a_n^3(t)\,\psi_n(x,y).
\end{aligned}
\tag{4.1}
$$

For the given set of the base functions $\{\psi_n\}$, $n = 1,\dots,N$ determined according to the FEM rules, at each instant of time t_k, $k = 0,\dots,M$ (where $t_k - t_{k-1} = \Delta t$ denotes an assumed time step) a set of coefficients $\{a_n^i\}_k$, $n = 1,\dots,3N$ is sought, where N is the number of the base functions. These coefficients will be determined with use of the three-point Lees method [11] according to the expression

$$
\begin{aligned}
\left\{a_n^1\right\}_{k+1} = &-[\mathbf{A}/3 + \mathbf{C}/2\Delta t]^{-1}\\
&\times\left[\mathbf{A}/3\,\{a_n^i\}_k + (\mathbf{A}/3 + \mathbf{C}/2\Delta t)\{a_n^i\}_{k-1} + b\right],
\end{aligned}
\tag{4.2}
$$

where $\mathbf{A}$ and $\mathbf{C}$ are the stiffness and the time coefficient matrices, respectively, determined according to the semi-discrete Galerkin method, see [12], p. 146.

The first Eq. (3.1) now takes the form

$$
-k_1\frac{\partial^2 u_x}{\partial x^2} - k_2\frac{\partial^2 u_x}{\partial y^2} - k_2\frac{\partial^2 u_y}{\partial y\partial x} - k_3\frac{\partial^2 u_y}{\partial x\partial y} + k_4\frac{\partial \mu}{\partial x} = 0,
\tag{4.3}
$$

where

$$
\begin{aligned}
k_1 &= 2M + A - \frac{\gamma_\Theta^2}{c_\Theta}, & k_2 &= M,\\
k_3 &= A - \frac{\gamma_\Theta^2}{c_\Theta}, & k_4 &= \frac{\gamma_\Theta}{c_\Theta^\rho}.
\end{aligned}
\tag{4.4}
$$

On suitable rearranging Eq. (4.3) can be written down in the form

$$
\frac{\partial}{\partial x}\sigma_{11} + \frac{\partial}{\partial y}\sigma_{12} = 0.
\tag{4.5}
$$

The form of Eq. (4.3) serves to calculate those coefficients of the stiffness matrix $\mathbf{A}$ that form the rows numbered $3j - 2$, where $i, j = 1, 2, \dots, 3N$.

Particular terms are calculated by means of the following expressions:

$$
\begin{aligned}
A(3j-2,\,3i-2) &= k_1 \int_G \frac{\partial \psi_j}{\partial x}\frac{\partial \psi_i}{\partial x}dv + k_2 \int_G \frac{\partial \psi_j}{\partial y}\frac{\partial \psi_i}{\partial y}dv,\\
A(3j-2,\,3i-1) &= k_2 \int_G \frac{\partial \psi_j}{\partial y}\frac{\partial \psi_i}{\partial x}dv + k_3 \int_G \frac{\partial \psi_j}{\partial x}\frac{\partial \psi_i}{\partial y}dv,\\
A(3j-2,\,3i) &= k_4 \int_G \frac{\partial \psi_j}{\partial x}\psi_i\, dv.
\end{aligned}
\tag{4.6}
$$

The form of Eq. (4.5) clearly shows that the stress boundary conditions (3.2) for $x = \pm L$ can be realized as natural conditions for an appropriate Galerkin form. In a similar manner the expressions for the stiffness matrix elements in the rows numbered $3j - 1$ will be found accompanied by the stress boundary conditions at the sides $y = \pm H$. These magnitudes enter the second Eq. (4.2).

The stiffness matrix elements in the $3j$-th rows have the form

$$
\begin{aligned}
A(3j,\,3i-2) &= A(3j-2,\,3i-1) = 0,\\
A(3j,\,3i) &= K \int_G \frac{\partial \psi_j}{\partial x}\frac{\partial \psi_i}{\partial x}dv + K \int_G \frac{\partial \psi_j}{\partial y}\frac{\partial \psi_i}{\partial y}dv.
\end{aligned}
\tag{4.7}
$$

The boundary conditions (3.2) for the moisture outflow are not natural conditions. Therefore, the Galerkin form of equation $(3.1)_3$ should by supplemented with suitable integrals over the boundary of the region. For instance, for $x = L$ we have

$$
\left.\frac{\partial \mu}{\partial x}\right|_{x=L} = -\alpha_m/\Lambda_m\,(\mu - \mu_a)\,. \tag{4.8}
$$

To satisfy this boundary condition it appears necessary to introduce into the rows $3j$ of the stiffness matrix an additional term

$$
A(3j,\,3i)' = A(3j,\,3i) + K\alpha_m \int_\Gamma \psi_j \psi_i\, ds. \tag{4.9}
$$

The components of the free terms vector in the relationship (4.2) is also altered according to the expression

$$
b(3j)' = b(3j) - \mu_a K \alpha_m \int_\Gamma \psi_j\, ds. \tag{4.10}
$$

For the time coefficient matrix **C** the following relationships are applicable: the rows $3j-2$ and $3j-1$ have all vanishing terms, while the rows $3j$ have the terms:

$$
\begin{aligned}
C(3j, 3i-2) &= k_6 \int_G \psi_j \frac{\partial \psi_i}{\partial x} dv, \\
C(3j, 3i-1) &= k_6 \int_G \psi_j \frac{\partial \psi_i}{\partial y} dv, \\
C(3j, 3i) &= \int_G \psi_j \psi_i \, dv.
\end{aligned} \tag{4.11}
$$

Let us notice that the symmetry of the boundary conditions (3.2) enables only one quarter of the domain $(-L, L) \times (-H, H)$ to be considered, for instance the domain $(0, L) \times (0, H)$, remembering the symmetry with respect to the $0X$ and $0Y$ axes.

5. Numerical examples

The above procedure to solve the initial-boundary problem was employed to analyse the drying process of a prismatic bar whose rectangular cross-section had the dimensions $0.2\,\mathrm{m} \times 0.1\,\mathrm{m}$. The following set of material constants, taken from the literature on the subject [9, 10] were assumed:

$$
\begin{aligned}
A &= 10^9\,[\mathrm{N/m^2}], & M &= 6.25 \cdot 10^8\,[\mathrm{N/m^2}], \\
\Lambda_m &= 6.04 \cdot 10^{-7}[\mathrm{kg\ s/m^3}], & c_\Theta &= 6.6 \cdot 10^6\,[\mathrm{J/m^3}], \\
\alpha_\Theta &= 3.0 \cdot 10^{-5}, & \alpha_m &= 8.6 \cdot 10^{-5}\,[\mathrm{kg\,s/m^4}], \\
\rho_0 &= 1200\,[\mathrm{kg/m^3}], & \mu_a &= 40\,[\mathrm{J/kg}], \\
\mu_0 &= 100\,[\mathrm{J/kg}].
\end{aligned}
$$

Due to the exchange of spatial variables the problem was reduced to the rectangular domain 2×1. The rectangle was divided into 128 rectangular elements, each having 16 base functions. These were assumed in the form of bi-cubic Hermite's functions ([12], pp. 53–55). The time step Δt was equal to 1 s. Eventually, the problem consisted in the solution of a linear system of equations in 1836 unknowns for each time instant t_k. A decomposition into triangular matrices was used. The time-consuming triangularization of the

matrix $[\mathbf{A}/3 + \mathbf{C}/2\,\Delta t]$ was made only once. Next, for each step after the modification of the right-hand side of Eq. (4.2) all that was necessary was a rapid back-substitution and forward-substitution. The above method was used as less time-consuming than the iterative method ([13], pp. 142–153).

6. Numerical results

The results of calculations are visualized diagrammatically for three time instants $t_1 = 75\,\mathrm{s}$, $t_2 = 2.5\,\mathrm{min}$, $t_3 = 7.5\,\mathrm{min}$. Contour lines for the moisture potential at the instant t, in the whole considered region $(-L, L)\times(-H, H)$, are shown in Fig.1. A relevant quarter of the rectangle is also shown. All

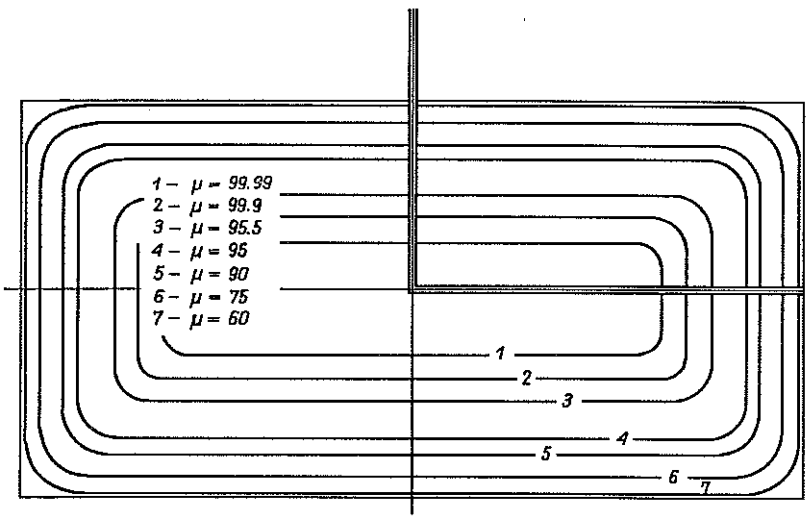

Fig. 1. Distribution of the moisture potential [J/kg] in the whole region at the instant $t_1 = 75\,\mathrm{s}$.

the further results will be given for this particular quarter (due to double symmetry of the domain in question). Contour lines for the moisture potential at the instants t_2 and t_3 are shown in Fig. 2. What should be stressed here is a movement of the lines of lower potential inwards as well as a change of their shapes as a result of the process becoming two-dimensional. These effects well agree with the intuition.

Displacements in the x-direction at the instant t_1 are depicted in Fig. 3 by means of suitable contour lines. At all the points of the region a shrinkage took place in the x-direction; it was larger near the edge where the moisture

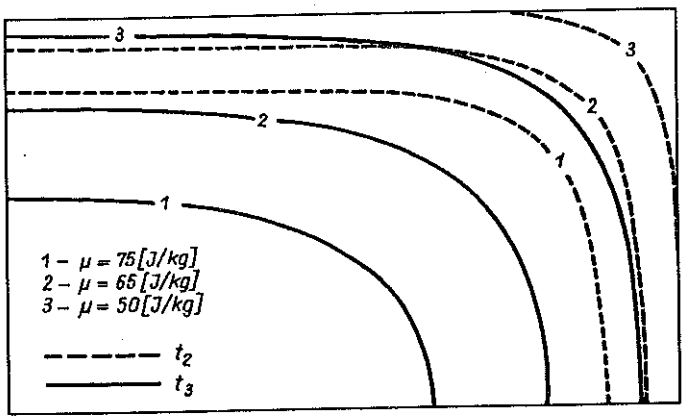

FIG. 2. Contour lines of the moisture potential in a quarter of the region at the instants $t_2 = 2.5$ min and $t_3 = 7.5$ min.

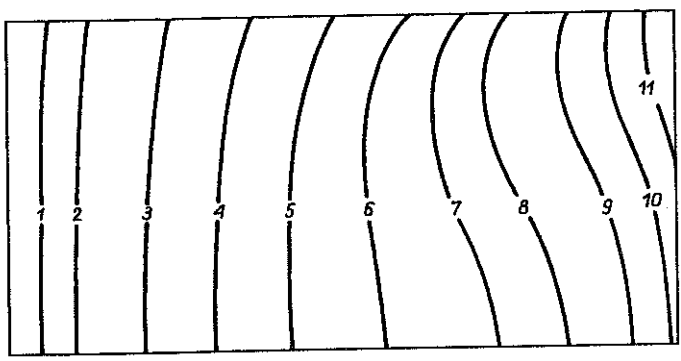

FIG. 3. Displacement contour lines $u_x \times 10^9$ [m] at the instant $t_1 = 75$ s.

1) $u_x = -1$, 2) $u_x = -2$, 3) $u_x = -4$,
4) $u_x = -6$, 5) $u_x = -8$, 6) $u_x = -10$,
7) $u_x = -12$, 8) $u_x = -14$, 9) $u_x = -18$,
10) $u_x = -22$, 11) $u_x = -26$.

content was considerably decreased. Displacements u_y at the instant t_1 in the y-direction are shown in Fig. 4. Unexpectedly enough, a certain swelling occurs here, i.e. positive displacements inside the region exist despite a decrease of moisture content in the whole rectangle. It is this very shape of the region that causes the observed effect; shrinkage on the shorter side and on the longer side lead to some different "resultant forces" of shrinkage. This effect is observed to be less pronounced at the instant t_2 and to disappear at the instant t_3 when all the displacements become negative. No such effects are visible for a square drying domain whose characteristics are given in Fig. 5.

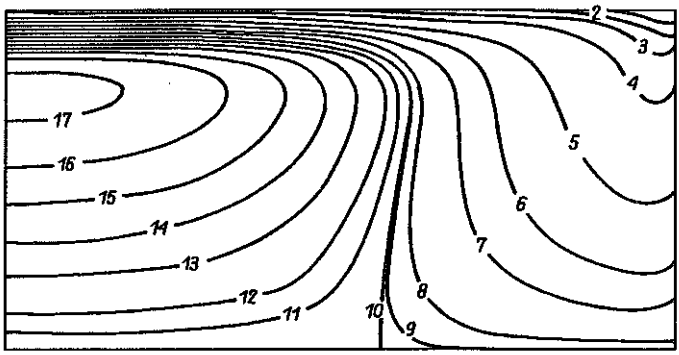

FIG. 4. Displacement contour lines $u_y \times 10^9$ [m] at the instant $t_1 = 75$ s.

1)	$u_y = -10$,	2)	$u_y = -8$,	3)	$u_y = -6$,
4)	$u_y = -4$,	5)	$u_y = -2$,	6)	$u_y = -1$,
7)	$u_y = -0.5$,	8)	$u_y = -0.1$,	9)	$u_y = -0.01$,
10)	$u_y = 0$,	11)	$u_y = 0.1$,	12)	$u_y = 0.2$,
13)	$uy = 0.4$,	14)	$u_y = 0.6$,	15)	$u_y = 0.8$,
16)	$u_y = 1.0$,	17)	$u_y = 1.2$.		

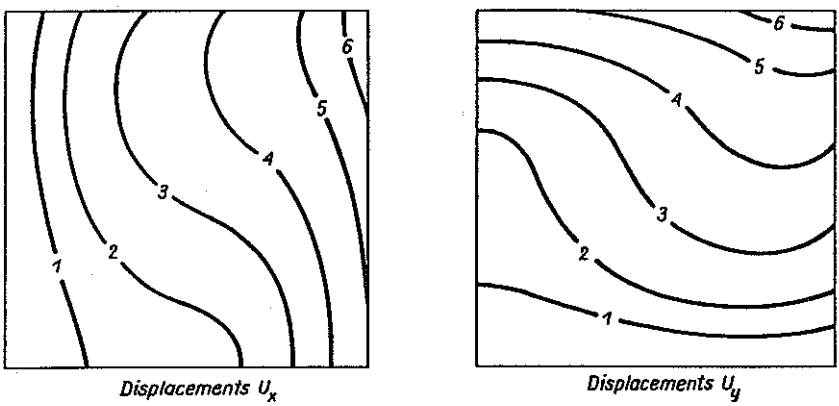

FIG. 5. Displacement contour lines u_x, $u_y \times 10^9$ [m] at the instant $t_1 = 75$ s in a square bar $2L \times 2L$.

1)	$u_i = -0.5$,	2)	$u_i = -1$,	3)	$u_i = -2$,
4)	$u_i = -4$,	5)	$u_i = -8$,	6)	$u_i = -12$.

The distributions of the moisture potential along the x- and y-directions at the instant t, are depicted in Fig. 6. Suitable dimensionless axes x/L and y/L are used. Drop in the moisture potential along the x-axis is larger what leads to also larger shrinkage in the same direction. The stresses generated by the shrinkage result in some swelling of the dried material inside the

domain and its positive displacements in the direction of least resistance, i.e. in the y-direction.

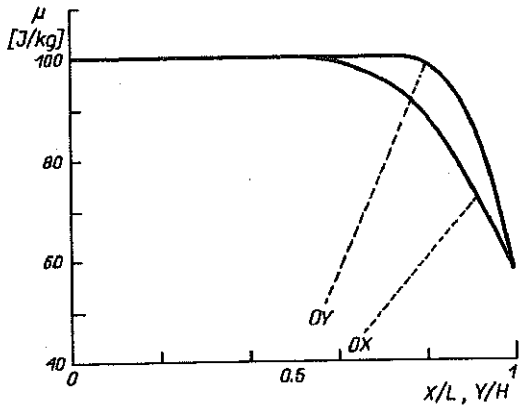

FIG. 6. Variation of the moisture potential along the axes $0X$ and $0Y$ at the instant $t_1 = 75\,\mathrm{s}$.

Let us now analyse the accompanying stresses. Contour lines of the stresses σ_{12} at the instant t_1 are seen in Fig. 7a. As expected, the shearing stresses in almost the whole region are negative. The existence of a small island of positive stresses with small values is a result of the same effect that was observed for the displacements u_y. Positive σ_{12} stresses decrease at the instant t_2 and completely disappear at the instant t_3, Figs. 7b, 7c. Moreover, along with the continuing process of drying accompanied by a decrease and equalization of the moisture content, the absolute values of shearing stresses diminish and corresponding contour lines smooth out.

Figures 8a and 8b shows the control lines of the stresses at the instants t_1 and t_3; Fig. 9 depicts the stresses σ_{22} at the instant t_2. Large tensile stresses along the sides of the domain parallel to the stress vector are observed together with compressive stress inside the rectangle.

The most dangerous for the drying material are the normal stresses. The diagram 10 in Fig. 8 shows the stresses σ_{11} along the X-direction and range $(0, L)$ for three time instants t_1, t_2 and t_3. This diagrams are similar to those obtained for the one-dimensional case (see [10]).

Figure 9 shows the contour lines of the stresses σ_{11} at the instants t_1 and t_3; Fig. 10 depicts the stresses σ_{22} at the instant t_2. Large tensile stresses along the sides of the domain parallel to stress vector are observed together with compressive stresses inside the rectangle.

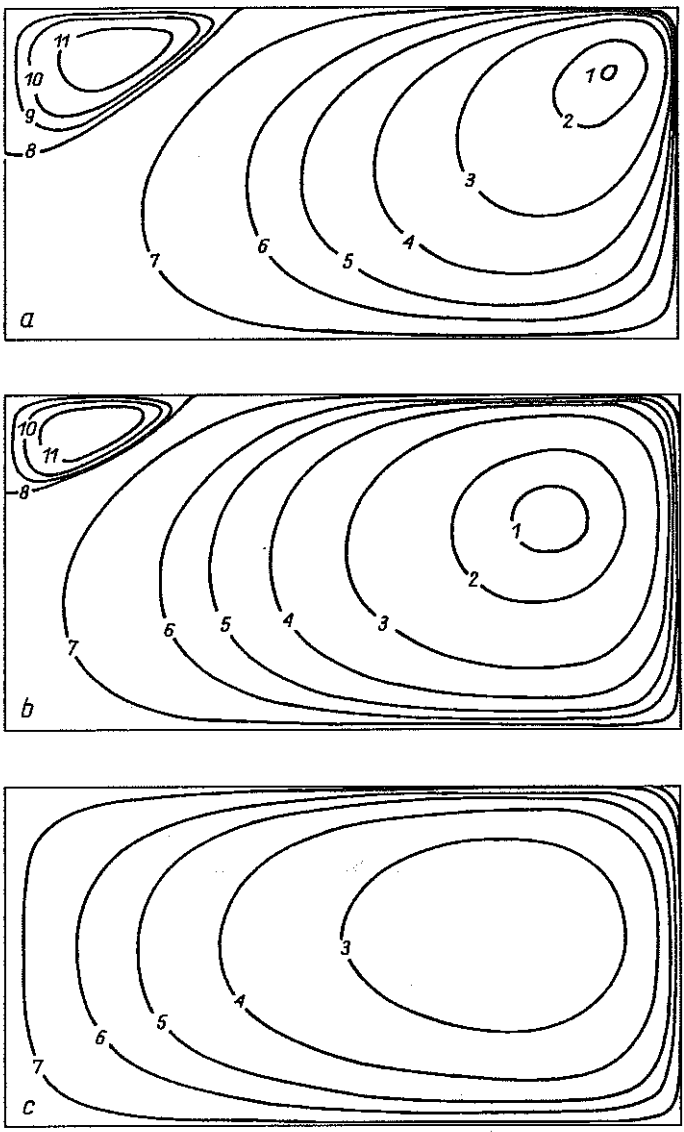

FIG. 7. σ_{12} stress contour lines at the instants:
a) $t_1 = 75$ s, b) $t_2 = 2.5$ min, c) $t_3 = 7.5$ min.

1) $\sigma_{12} = -100$, 2) $\sigma_{12} = -80$, 3) $\sigma_{12} = -40$,
4) $\sigma_{12} = -20$, 5) $\sigma_{12} = -10$, 6) $\sigma_{12} = -5$,
7) $\sigma_{12} = -1$, 8) $\sigma_{12} = 0$, 9) $\sigma_{12} = -0.05$,
10) $\sigma_{12} = 0.1$, 11) $\sigma_{12} = 0.2$.

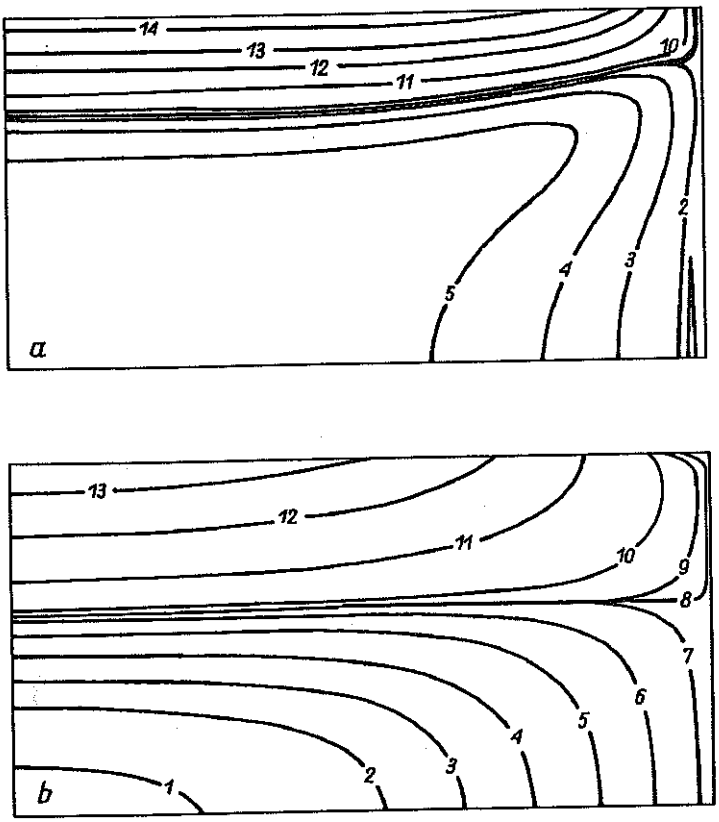

FIG. 8. Contour lines for the stresses $\sigma_{11} \times 10^{-9}$ [N/m^2] at the instants: a) $t_1 = 75$ s, b) $t_3 = 7.5$ min.

1) $\sigma_{11} = -160$, 2) $\sigma_{11} = -120$,
3) $\sigma_{11} = -90$, 4) $\sigma_{11} = -60$,
5) $\sigma_{11} = -30$, 6) $\sigma_{11} = -10$,
7) $\sigma_{11} = -1$, 8) $\sigma_{11} = 0$,
9) $\sigma_{11} = 1$, 10) $\sigma_{11} = 10$,
11) $\sigma_{11} = 60$, 12) $\sigma_{11} = 150$,
13) $\sigma_{11} = 250$, 14) $\sigma_{11} = 400$.

Movement of the line $\sigma_{11} = 0$ is shown in Fig. 11 for the three considered instants of time. This line travels towards the centre of the region and becomes straighter.

The contour lines of σ_{22} and σ_{12} at the instant t_1 for a square bar are depicted in Fig. 12. Similarly as for displacements and stresses, some anomalies caused by the anisotropy of the studied region tend to disappear.

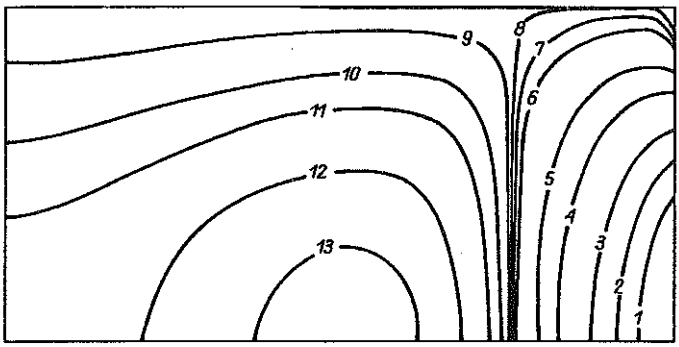

FIG. 9. Contour lines for the stresses $\sigma_{22} \times 10^{-9}$ [N/m^2] at the time $t_2 = 2.5$ min.

1) $\sigma_{22} = -120$, 2) $\sigma_{22} = -90$, 3) $\sigma_{22} = -60$,
4) $\sigma_{22} = -30$, 5) $\sigma_{22} = -15$, 6) $\sigma_{22} = -3$,
7) $\sigma_{22} = -1$, 8) $\sigma_{22} = 0$, 9) $\sigma_{22} = 1$,
10) $\sigma_{22} = 5$, 11) $\sigma_{22} = 10$, 12) $\sigma_{22} = 20$,
13) $\sigma_{22} = 3$.

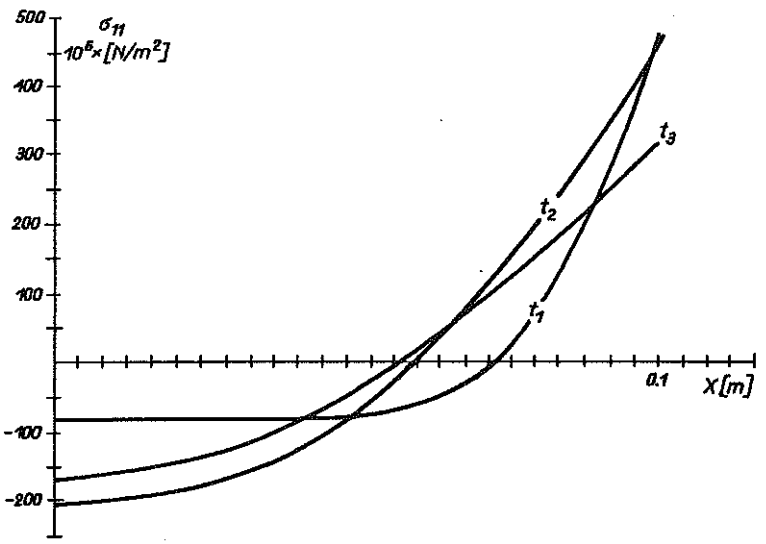

FIG. 10. σ_{11} stress contour lines along the axis $0X$ at the instants $t_1 = 75$ s, $t_2 = 2.5$ min, $t_3 = 7.5$ min.

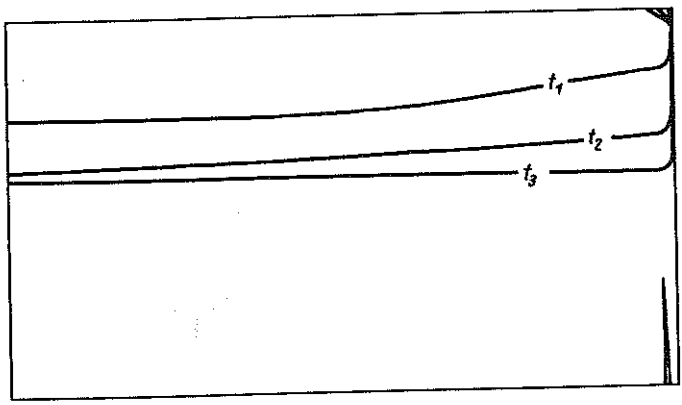

FIG. 11. Movement of the surface $\sigma_{11} = 0$ at the instants $t_1 = 75\,\text{s}$, $t_2 = 2.5\,\text{min}$, $t_3 = 7.5\,\text{min}$.

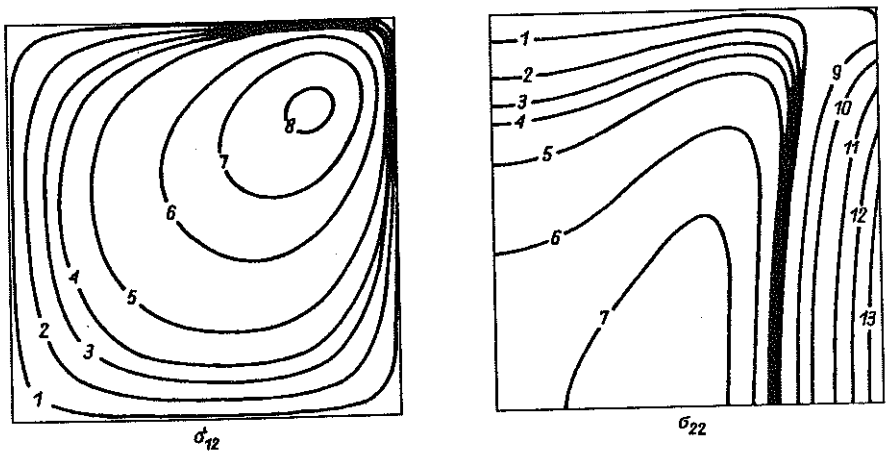

FIG. 12. Contour lines for the stresses σ_{12}, $\sigma_{22} \times 10^{-9}$ [N/m^2] at instant $t_1 = 75\,\text{s}$ in a square bar $2L \times 2L$.

1) $\sigma = -1$, 2) $\sigma = -5$, 3) $\sigma = -10$, 4) $\sigma = -15$,
5) $\sigma = -25$, 6) $\sigma = -50$, 7) $\sigma = -75$, 8) $\sigma = -100$,
9) $\sigma = 50$, 10) $\sigma = 100$, 11) $\sigma = 200$, 12) $\sigma = 300$,
13) $\sigma = 400$.

7. GENERAL CONCLUSIONS

The following conclusions can be drawn from the solved two dimensional problem of drying of a prismatic bar having a rectangular cross-section.

First, the obtained results agree with intuition and certain expectations resulting from experimental evidence. At the same time, the suitability

of the used model of the phenomenon and the method of its solutions are confirmed.

Second, the solution shows that appropriate theoretical considerations can enrich the knowledge on the phenomenon under consideration. At the first glance surprising results are obtained in the paper. However, they can be interpreted in a reasonable manner. The appearance of a subregion inside the whole studied domain in which local positive stresses occur (due to anisotropy of the shape of the dried body) would have been very difficult to discover experimentally.

Finally, the obtained results for $2D$ situation provide a number of additional pieces of information of a cognitive nature as compared with the unidimensional problem in [10]. These are: faster drying of corners and larger stresses in them, appearance of the field of maximum shearing stresses inside the considered domain and so on.

Since the material of the bar was assumed to be elastic and the numerical input data did not refer to any specific material, the presented results are rather of a qualitative character.

REFERENCES

1. M.ILIC, I.W.TURNER, *Drying of a wet porous material*, Appl. Math.Modelling, **10**, 2, 16–24, 1986.
2. M.ILIC, I.W.TURNER, *Convective drying of a consolidated slab of wet porous material*, Int. J. Heat Mass Transfer, **32**, 12, 2351–2362, 1989.
3. I.W.TURNER, M.ILIC, *Convective drying of a consolidated slab of wet porous material including the sorption region*, Int. Communications in Heat and Mass Transfer, **17**, 1, 39–48, 1990.
4. R.W.LEWIS, M.STRADA, G.COMINI, *Drying induced stresses of porous bodies*, Int. J. Numer. Meth. Engng., **11**, 1175–1164, 1977.
5. S.B.NASRALLAH, P.PERRE, *Detailed study of a model of heat and mass transfer during convective drying of porous media*, Int. J. Heat Mass Transfer, **31**, 5, 957–967, 1988.
6. CZ.STRUMIŁŁO, *Fundamentals of the theory and practice of drying* [in Polish], PWN, Warszawa 1970.
7. S.J.KOWALSKI, *Thermomechanics of constant drying rate period*, Arch. Mech., **39**, 3, 157–176, 1987.
8. S.J.KOWALSKI, *Thermomechanics of dried materials*, Arch. Mech. **42**, 2, 123–149, 1990.

9. S.J.KOWALSKI, G.MUSIELAK, *Problems of mathematical modelling of the drying process for wet porous-capillary media on an example of convective drying of a slab* [in Polish], Rozpr. Inżyn., **36**, 2, 239–252, 1988.

10. S.J.KOWALSKI, G.MUSIELAK, A.RYBICKI, *Shrinkage stresses in dried materials*, Engng. Trans., **40**, 1, 115–131, 1992.

11. M.LESS, *A linear three-level difference scheme for quasi-linear parabolic equations*, Maths. Comp., 20, 516–622, 1966.

12. A.R. MITCHELL, R.WAIT, *Finite element analysis and applications*, J. Wiley and Sons, 1985.

13. J.BJŐRCK, G.DOHLQUIST, *Numerical methods* [in Polish], pp. 179–185, PWN 1987.

POLISH ACADEMY OF SCIENCES
INSTITUTE OF FUNDAMENTAL TECHNOLOGICAL RESEARCH.

Received December 18, 1992.